The Thirteenth International Conference on Sensor Device Technologies and Applications
SENSORDEVICES 2022- Lisbon, Portugal

Room temperature metal oxides based gas sensors for detecting fish freshness

Kaidi Wu [a,b], Marc Debliquy [b], Chao Zhang [a]

a College of Mechanical Engineering, Yangzhou University, Yangzhou 225127, PR China
b Materials Science Department, Faculty of Engineering, University of Mons, 20 Place du Parc, Mons, Belgium

E-mail: kaidi.wu@student.umons.ac.be; wkdlights@gmail.com

Contents

Background

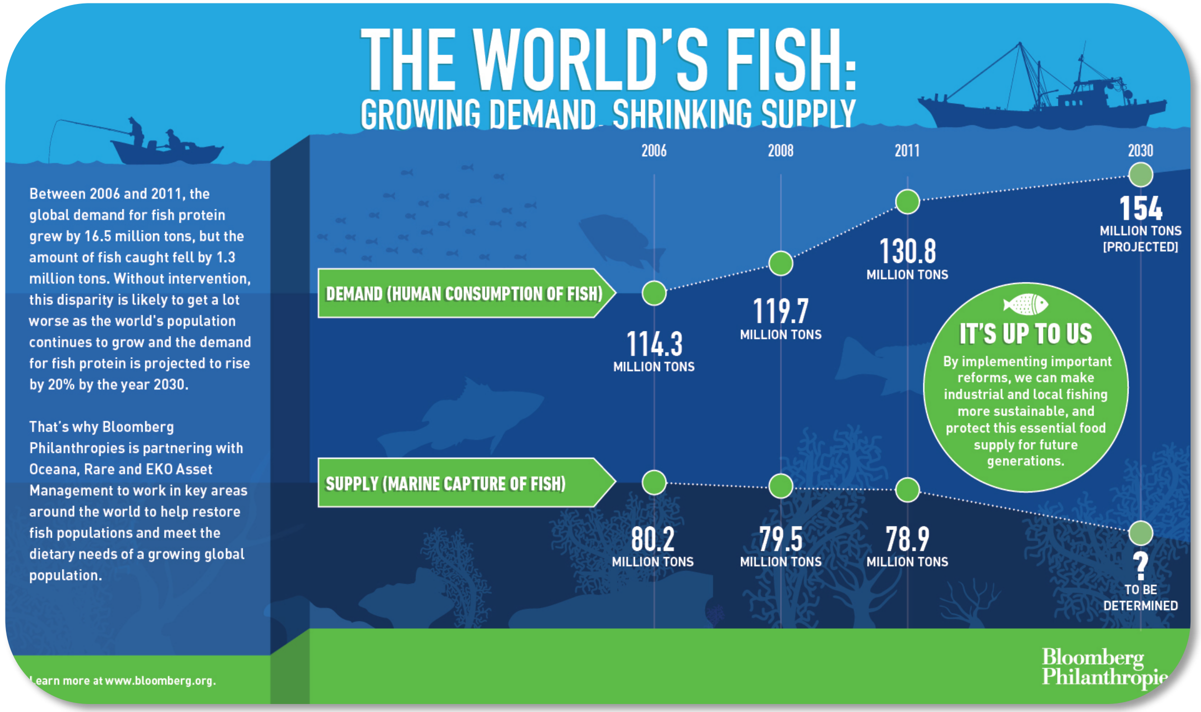

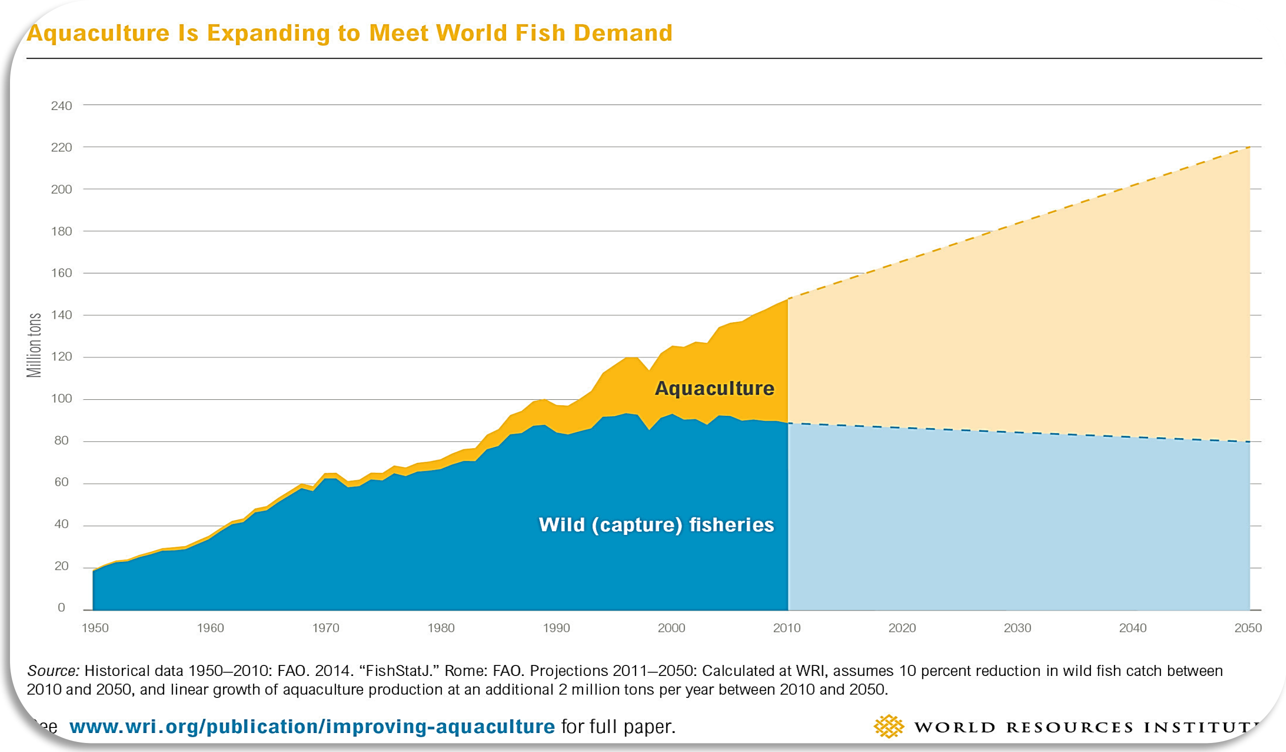

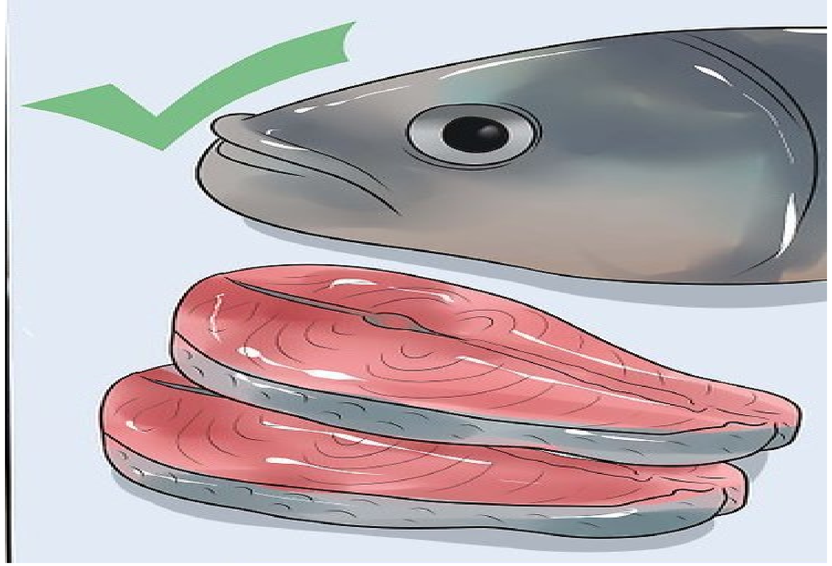

- Unsaturated fatty acid
- Soluble protein
- Dense connective tissue and fascia wrap
- Endogenous enzymes

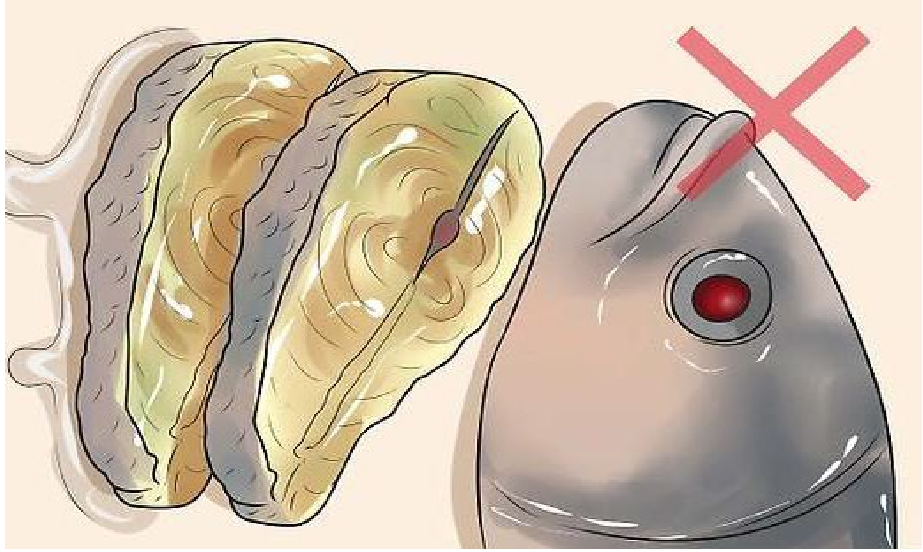

Fish freshness and food safety

Sensory testing

Professionals;

strong subjectivity

Physical and chemical analysis

High cost;

Difficult to operate;

Poor qualitative ability;

Frequent maintenance

Traditional methods（Destructive testing）

Detection and Assessment:

Rapid

Nondestructive

Low cost

Indicators: Released gases from spoiled fish

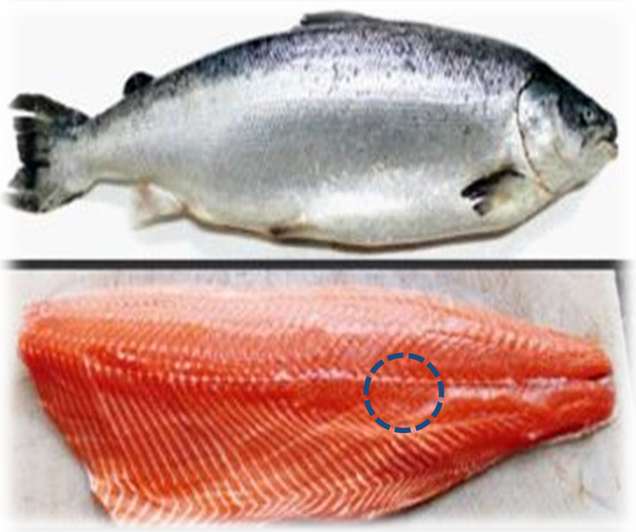

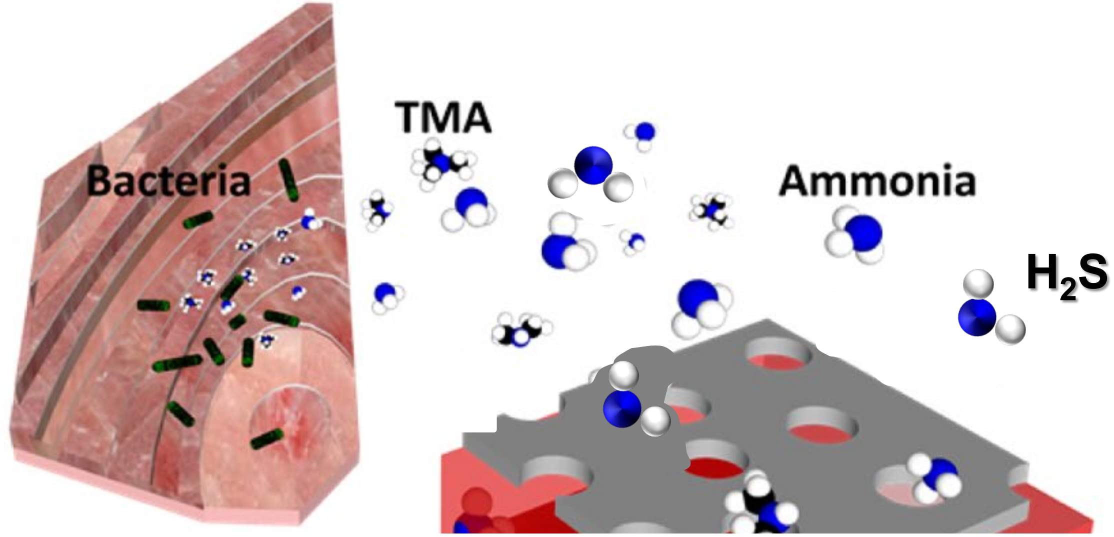

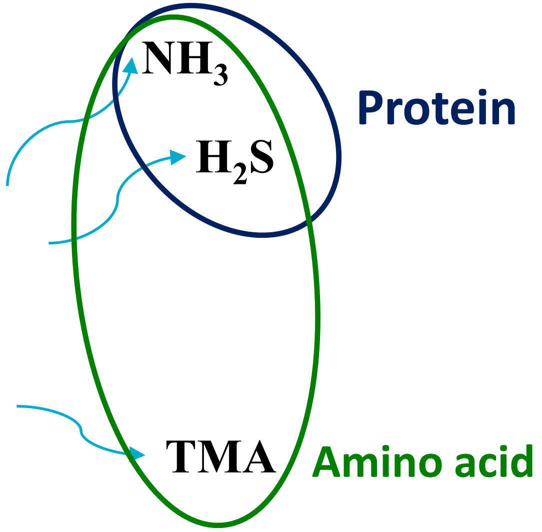

Reduced flavor

Food safety risks

Transportation

Storage

Features

Diversity

Complexity

Low concentration

Gas sensors

low working temperature

low detection limit

good selectivity

Introduction of Metal Oxides Semiconductor (MOS) gas sensors

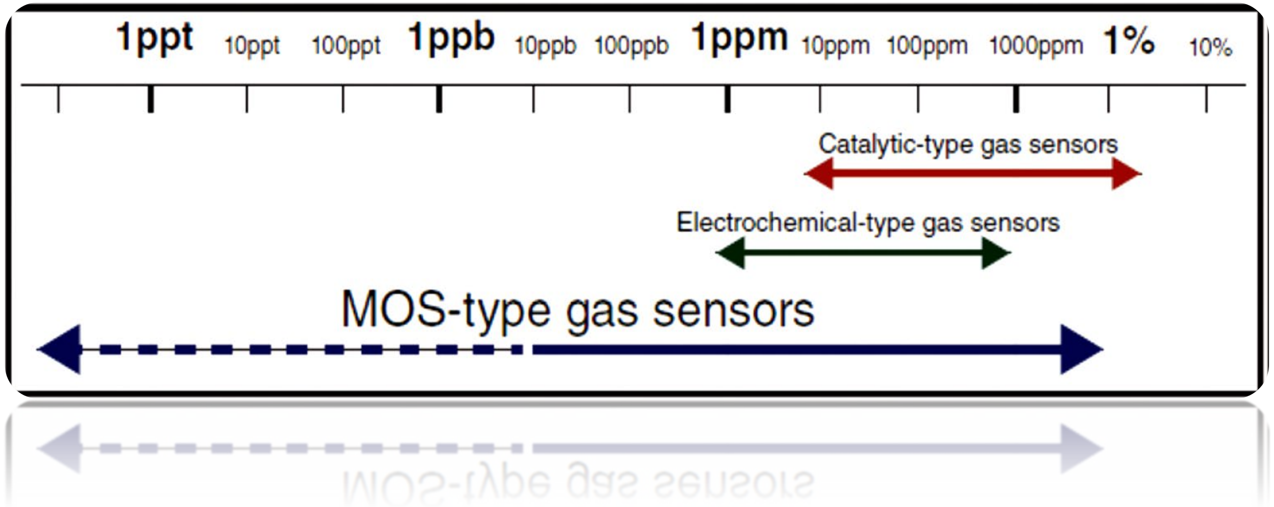

Gas concentration sensing range of several common gas sensors

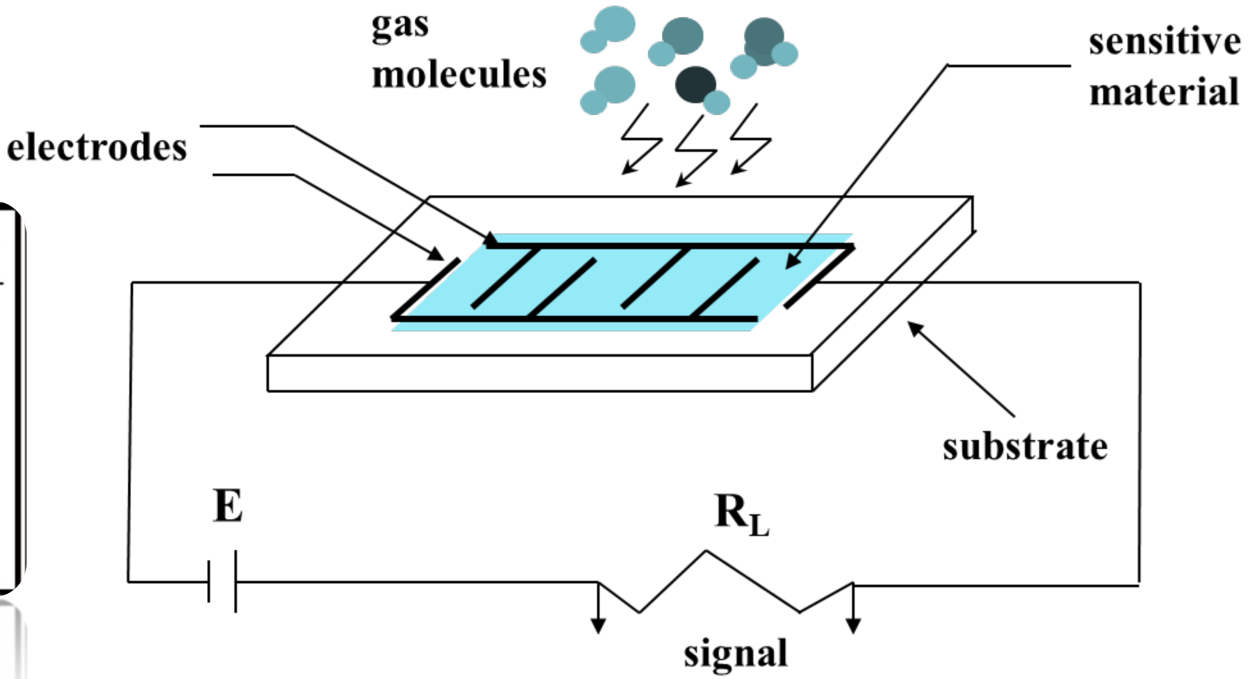

- Gas adsorption induces electrical conductivity variations $\Delta\sigma = f(C_{gas})$
- Resistance measurement = C_{gas} measurement

Main characteristics

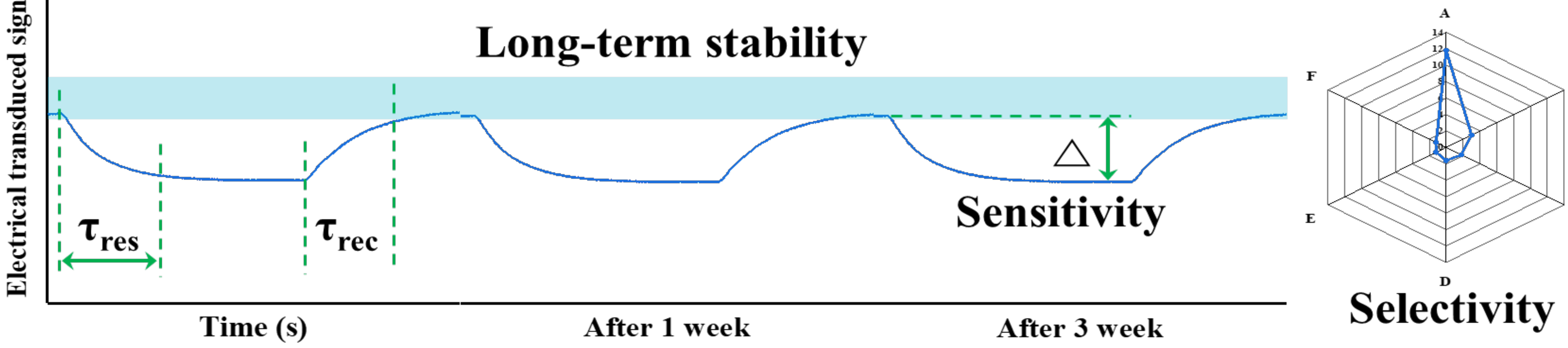

Working principles

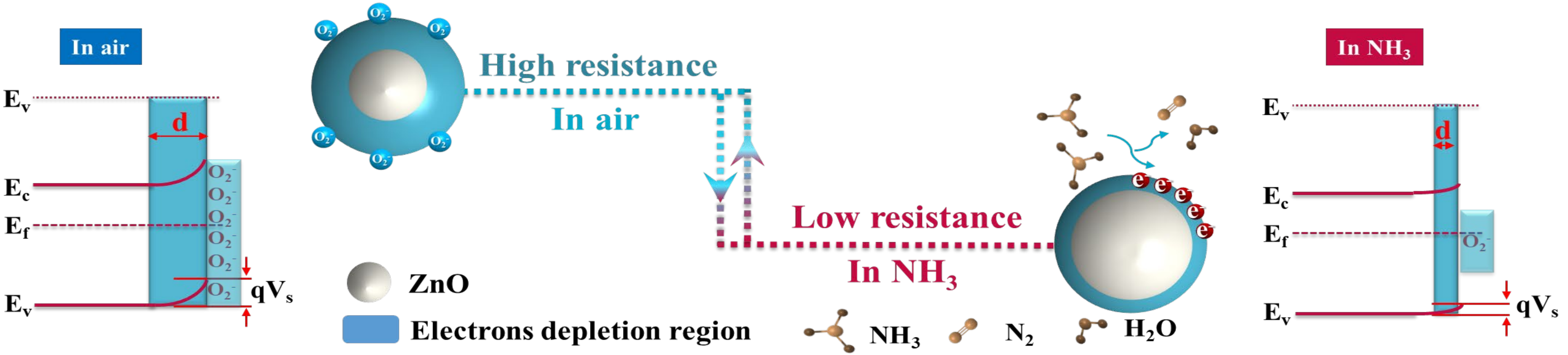

Contents

Gas sensor test system

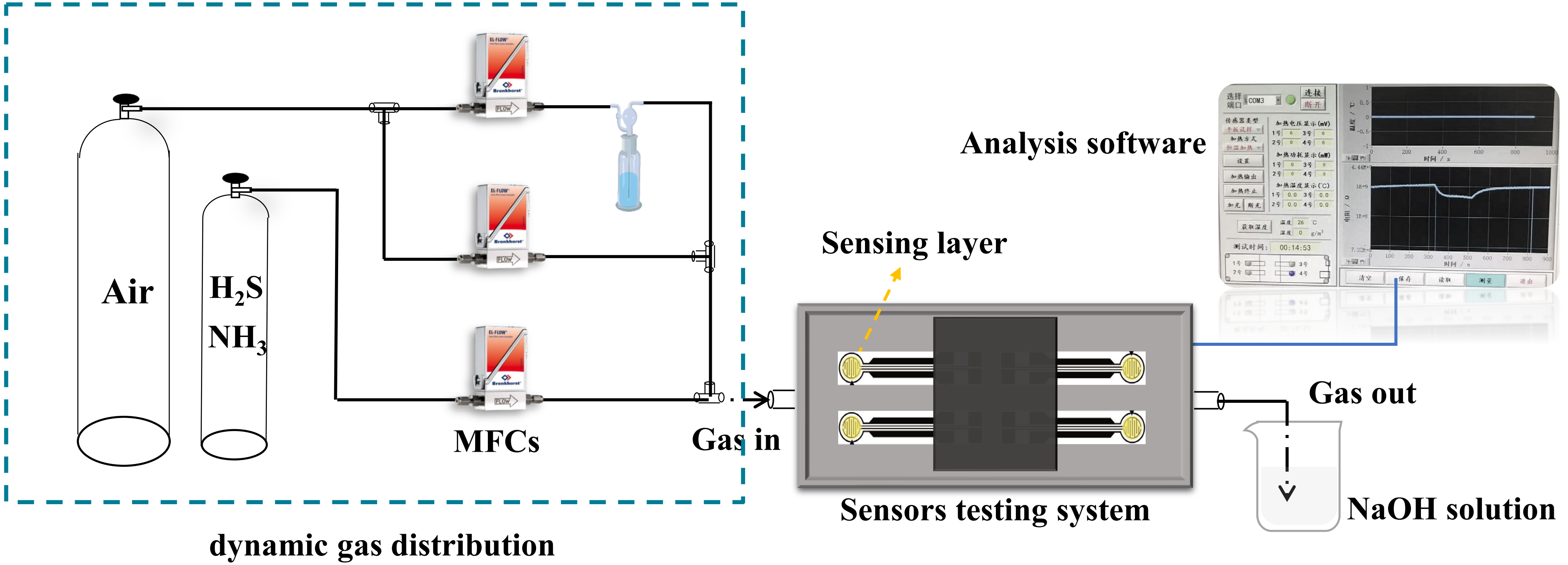

① WO_3-Bi_2WO_6 microflowers based H_2S sensor

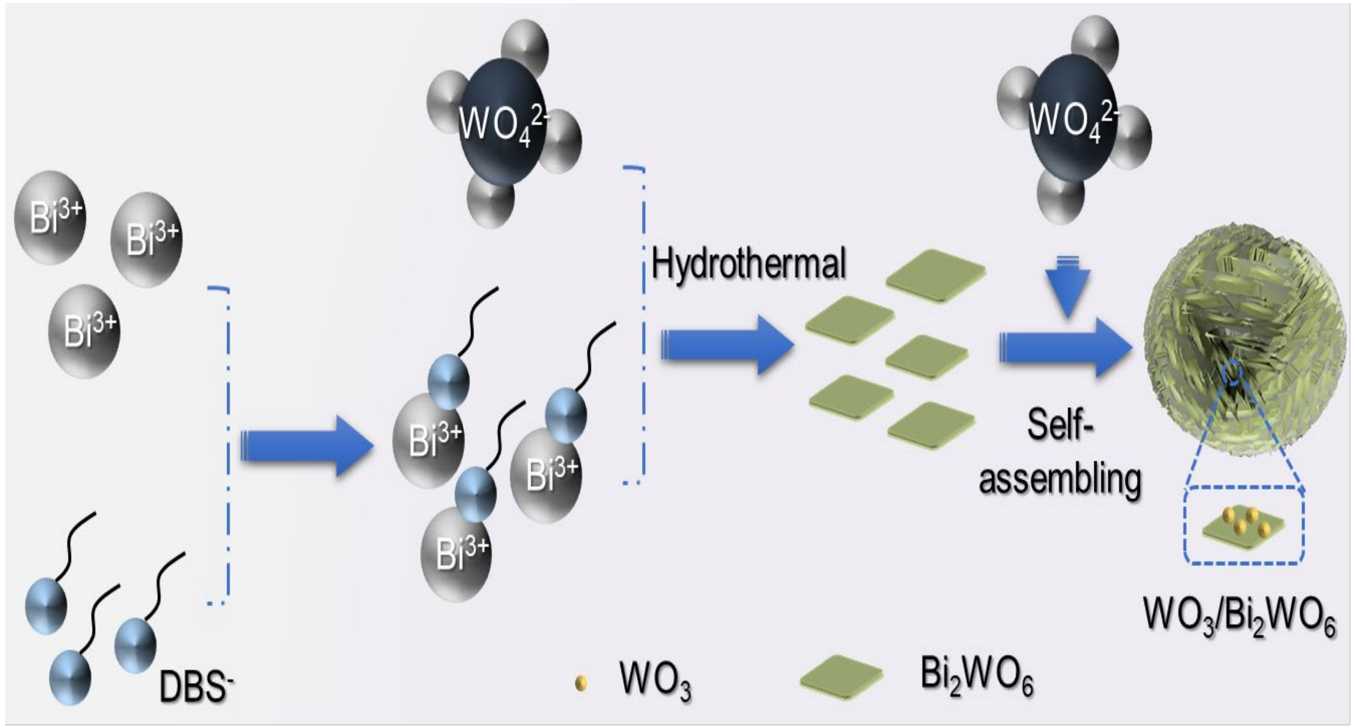

Scheme 1. Synthesis mechanism of pristine Bi_2WO_6 and WO_3-Bi_2WO_6.

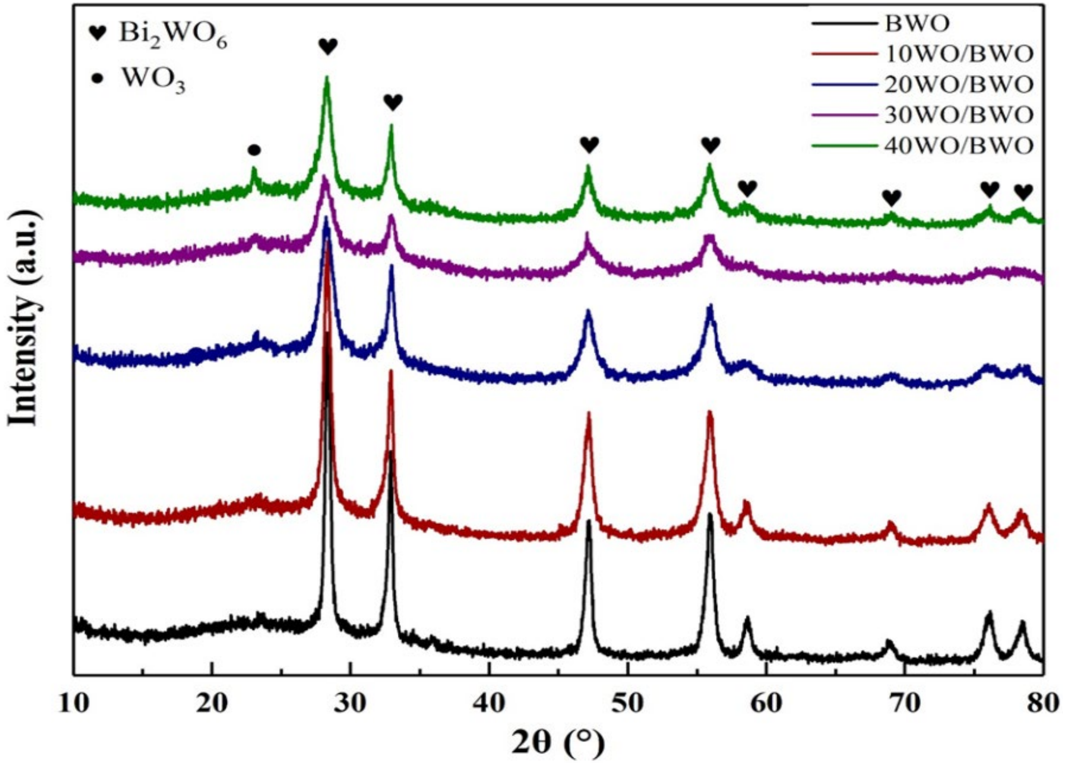

Fig. 1.1. X-ray Powder Diffraction (XRD) patterns of pure Bi_2WO_6 and WO_3-Bi_2WO_6 composites.

WO_3-Bi_2WO_6 microflowers based H_2S sensor

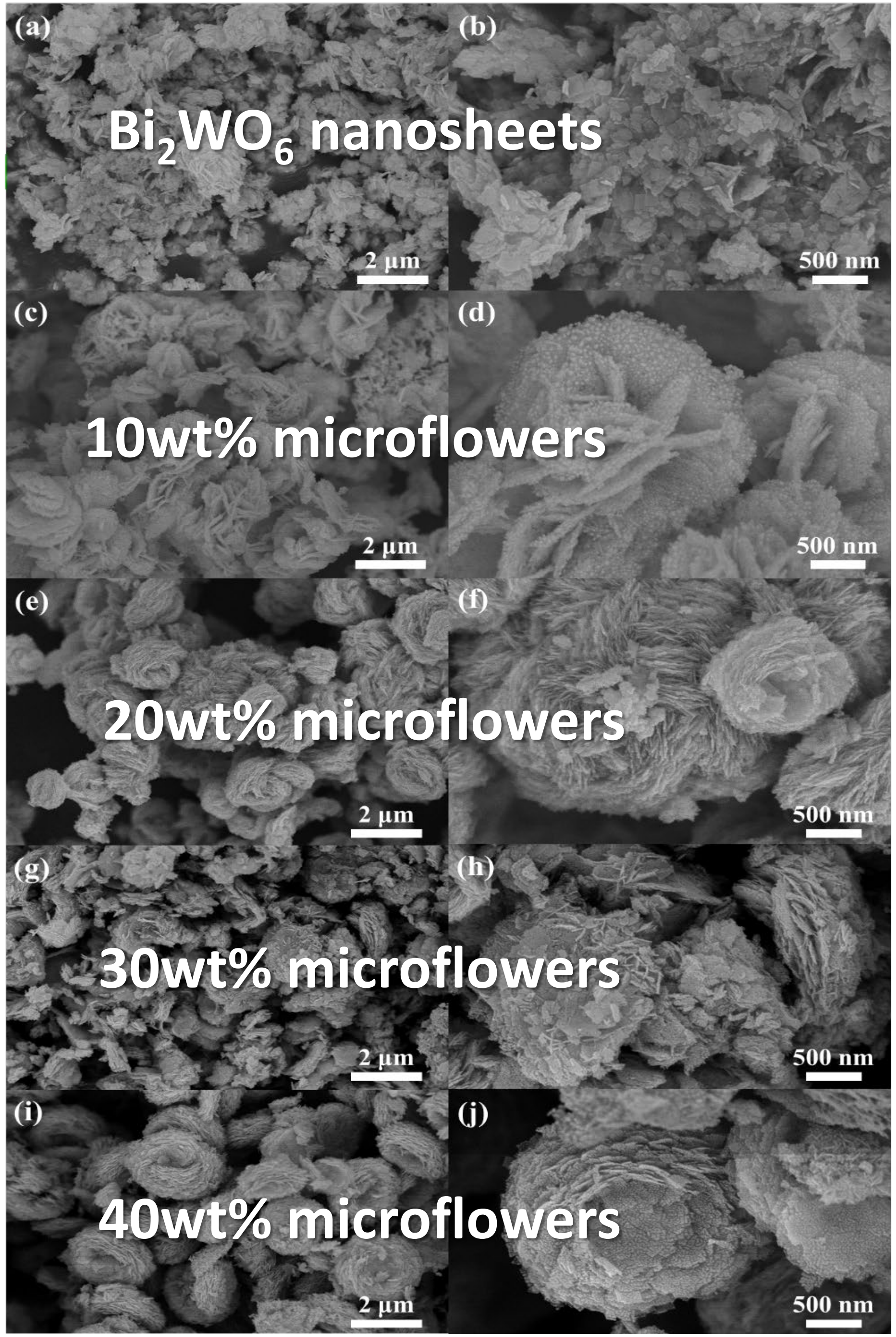

Fig. 1.2. Scanning electron microscope (SEM) images.

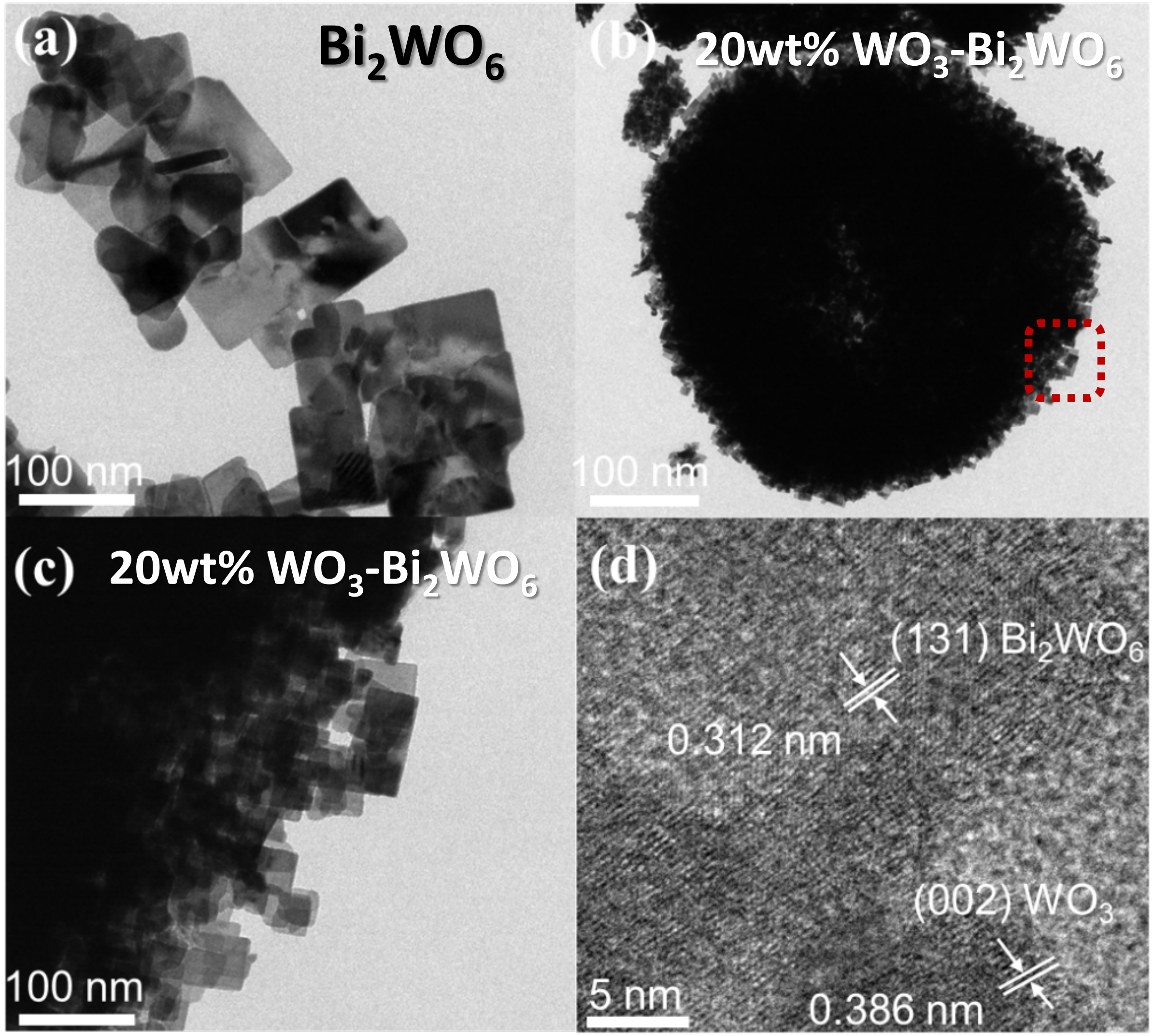

Fig. 1.3. Transmission electron microscope (TEM) images.

WO_3-Bi_2WO_6 microflowers based H_2S sensor

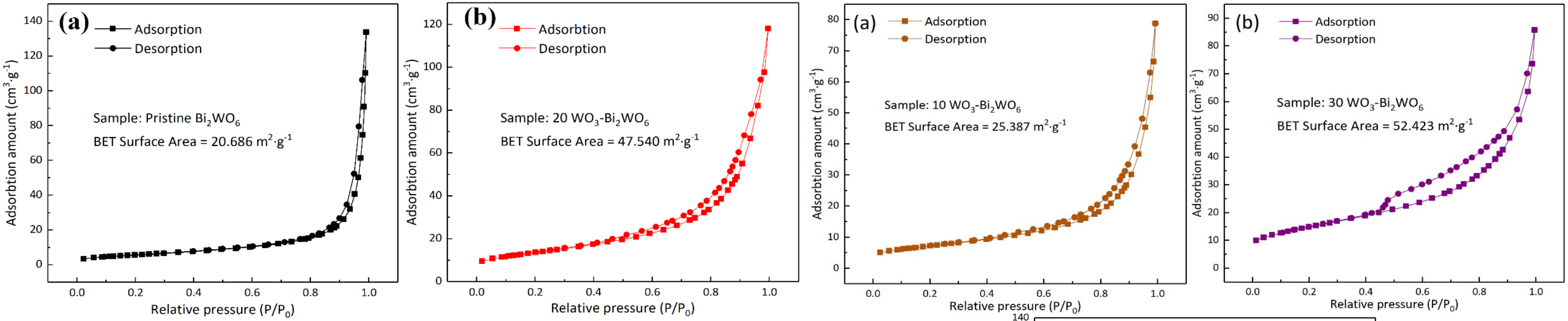

Sample	Specific Surface Area ($m^2 \cdot g^{-1}$)	Average Pore Size (nm)	Pore Volume ($cm^3 \cdot g^{-1}$)
Bi_2WO_6	20.685	37.068	0.192
10 WO_3-Bi_2WO_6	25.387	18.198	0.116
20 WO_3-Bi_2WO_6	47.540	14.127	0.168
30 WO_3-Bi_2WO_6	52.463	9.089	0.119
40 WO_3-Bi_2WO_6	42.787	18.033	0.193

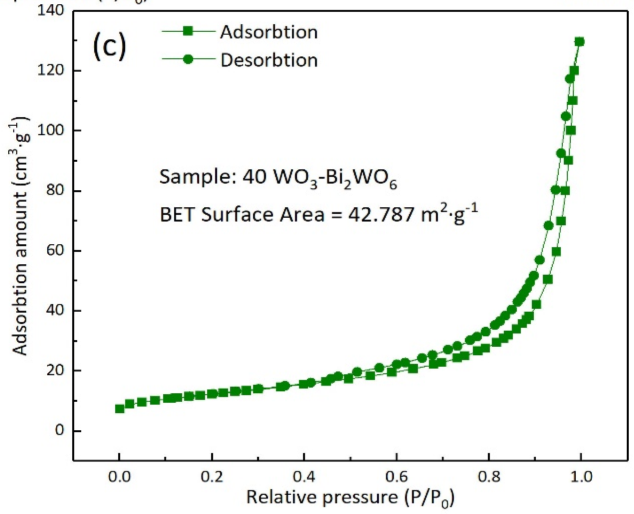

Fig. 1.4. N_2 adsorption/desorption isotherm curves.

Sensors evaluations

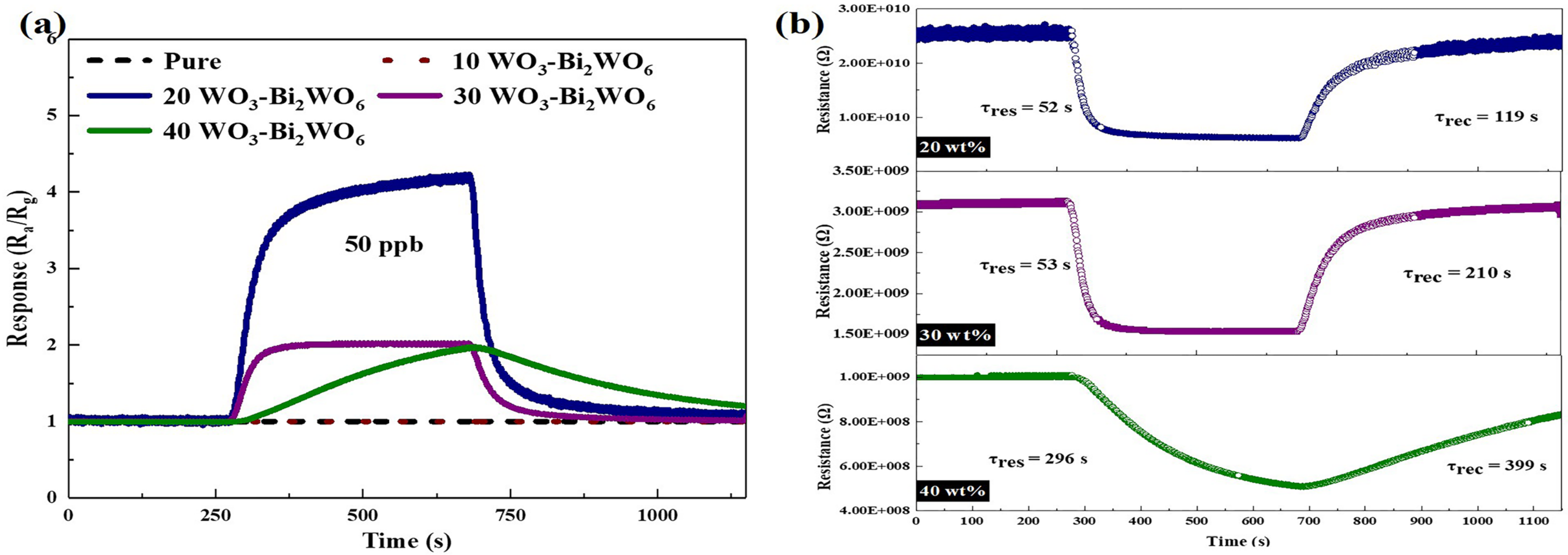

Fig. 1.5. (a) Responses to 50 ppb H_2S at room temperature; (b) dynamic response/recovery curves of 20/30/40 WO_3-Bi_2WO_6 to 50 ppb H_2S at room temperature.

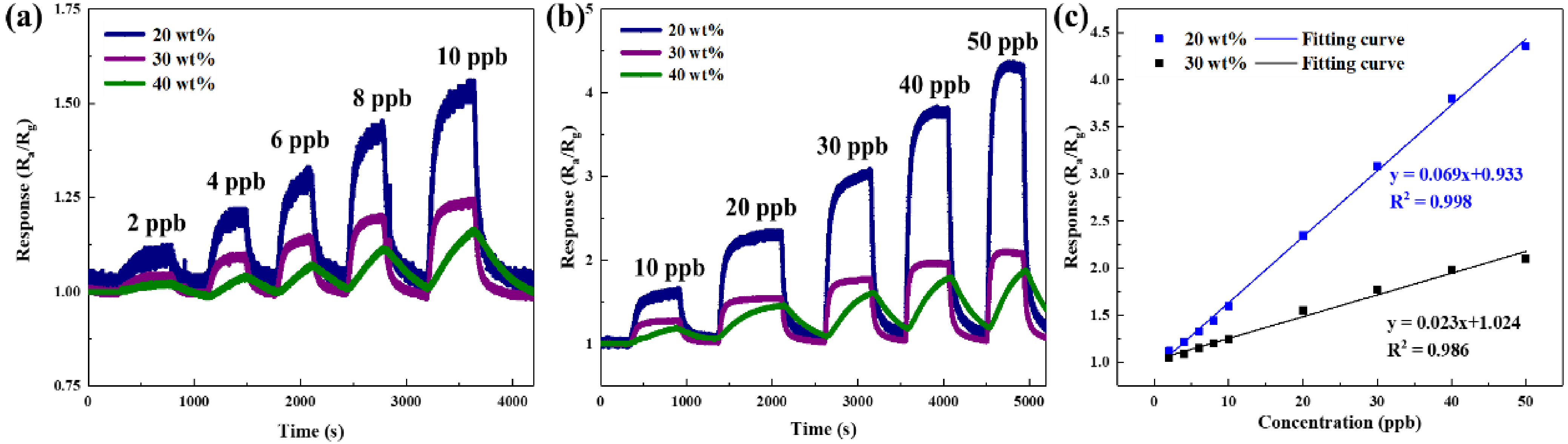

Fig. 1.6. (a, b) Dynamic sensing performance of three gas sensors to 2–50 ppb H_2S at room temperature; (c) response values and the fitted curves of three gas sensors versus H_2S concentration.

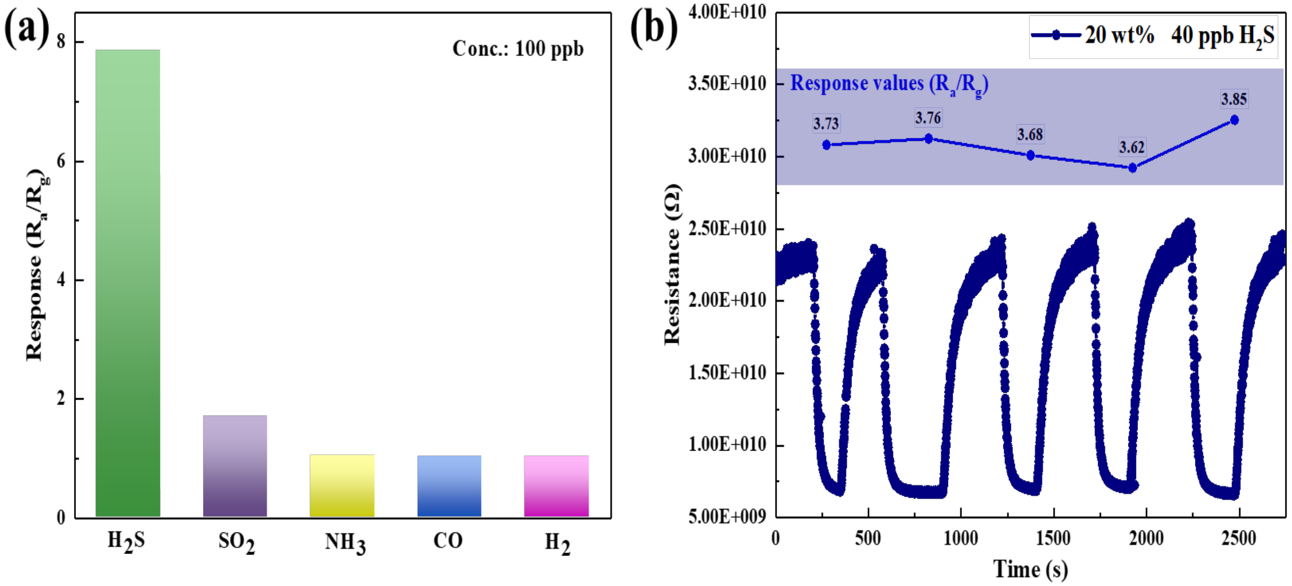

Fig. 1.7. (a) selectivity of 20 WO_3-Bi_2WO_6 to 100 ppb target gases; (b) effect of relative humidity on 20 WO_3-Bi_2WO_6 to 40 ppb H_2S.

Practical 1:

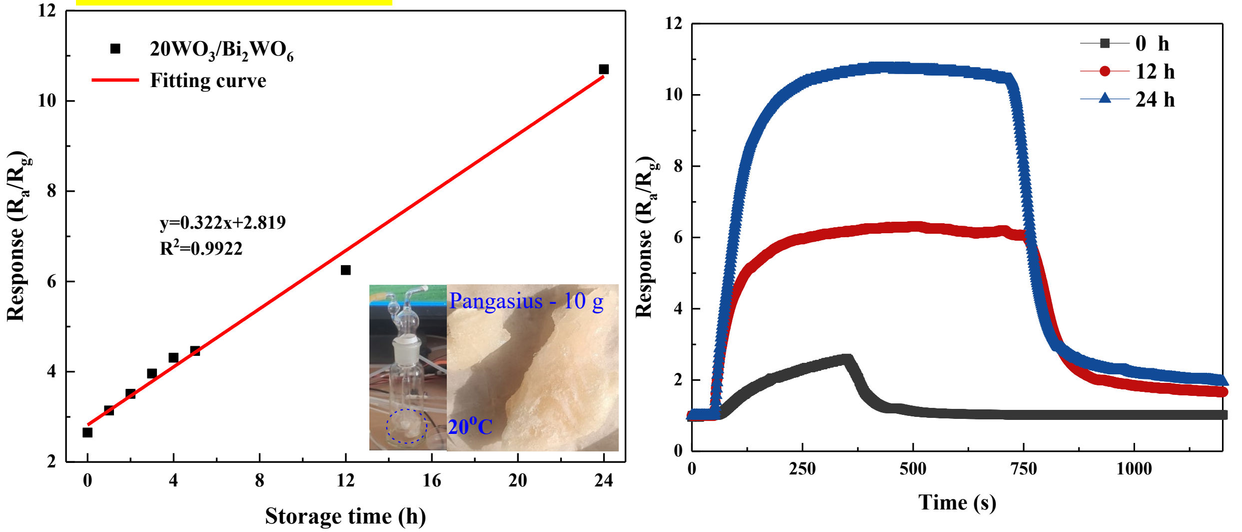

Fig. 1.8. Detecting the volatiles from 10 g Pangasius after storage for 0, 12 and 24 h.

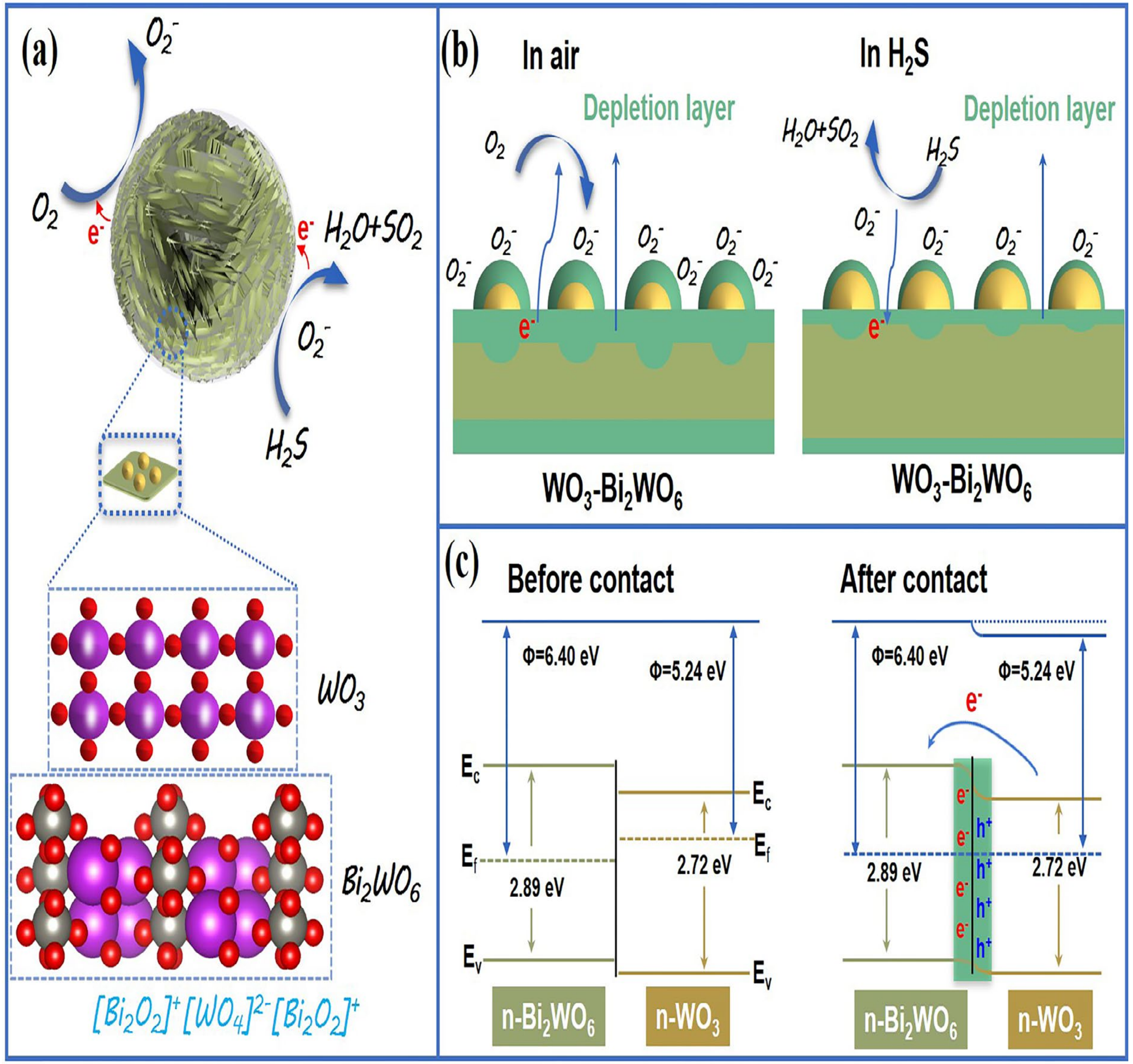

Fig. 1.9. (a, b) Schematic illustration of H_2S sensing mechanism and (c) Energy band diagram of WO_3-Bi_2WO_6 heterojunction structure.

② Ce-TiO_2 based NH_3 sensor

10 mL Tetrabutyl titanate

$Ce(NO_3)_3 \cdot 6H_2O$

30 mL ethanol

3 mL 5 mol/L HNO_3

→ Magnetically stirring 2 h → Microwave reactor

↓ 120°C 1 h 500W

Cooling down

↓ Centrifugation washing

↓ Drying 60°C, 6 h

Ce-TiO_2 nanocrystals

Microwave assisted hydrothermal synthesis

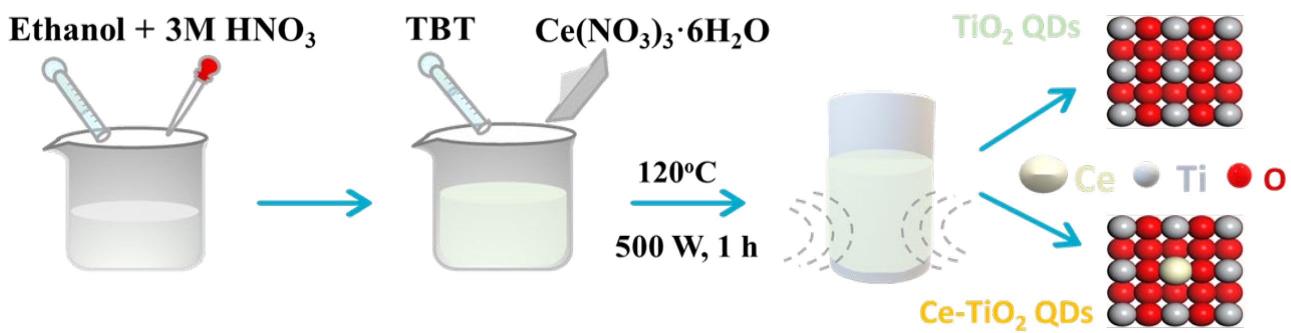

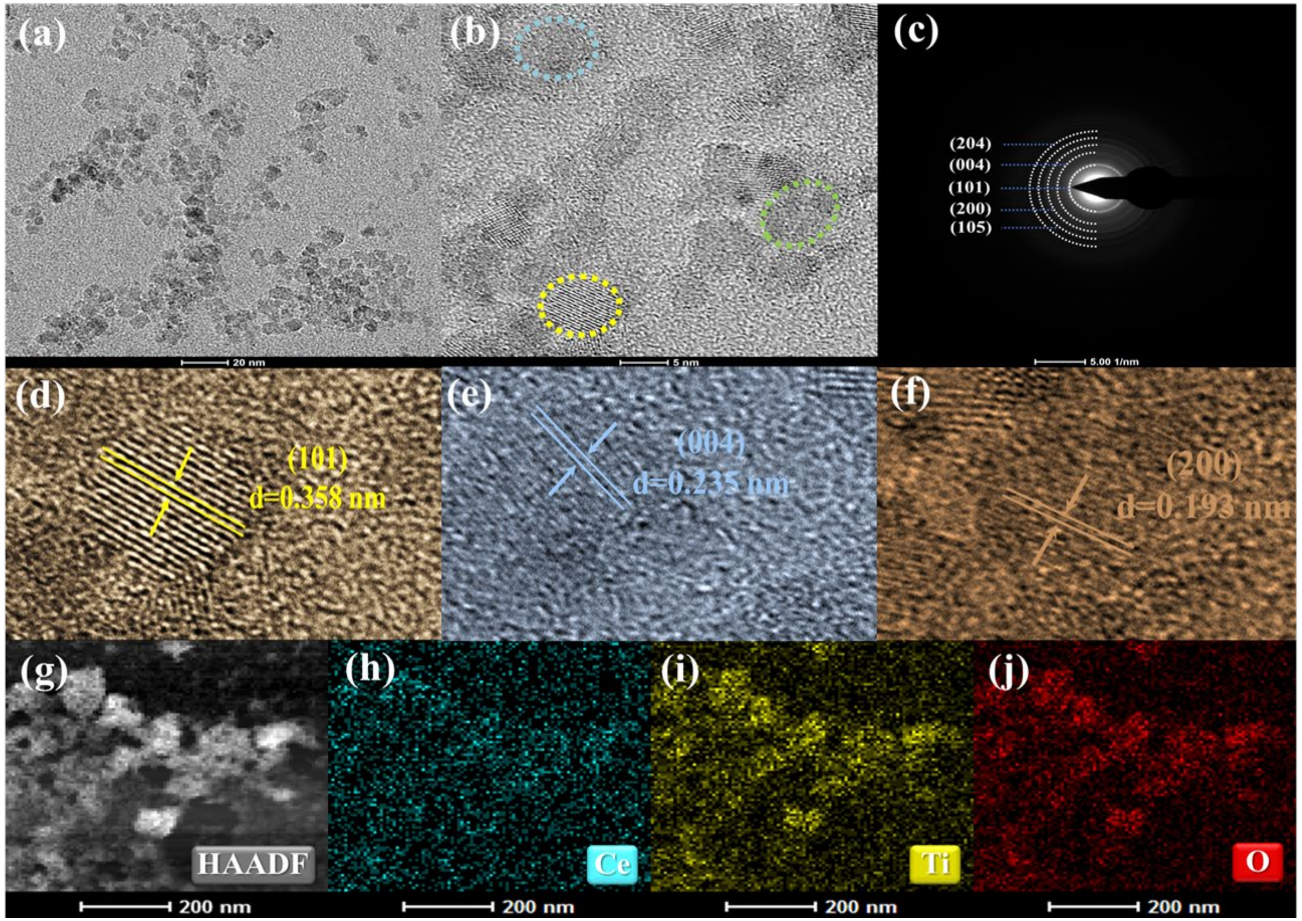

Nanostructure details

XRD and X-ray photoelectron spectroscopy (XPS)

Element chemical states

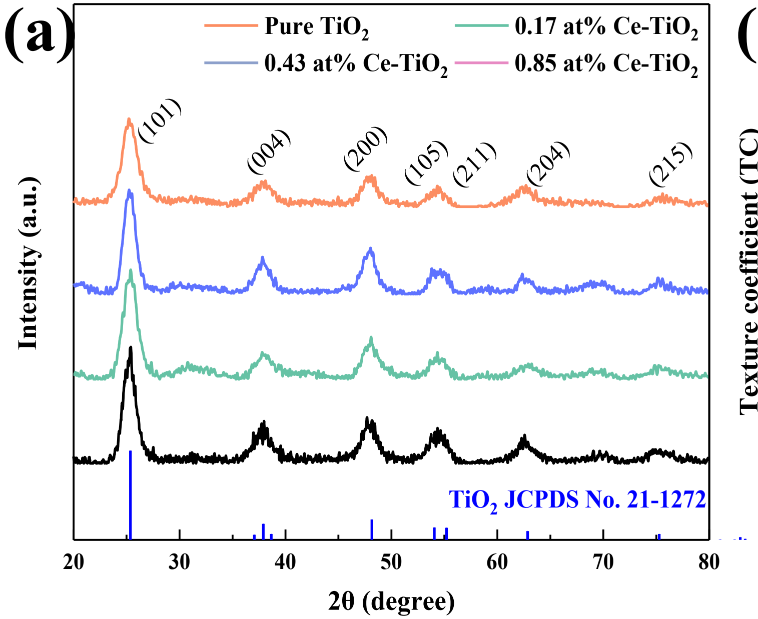

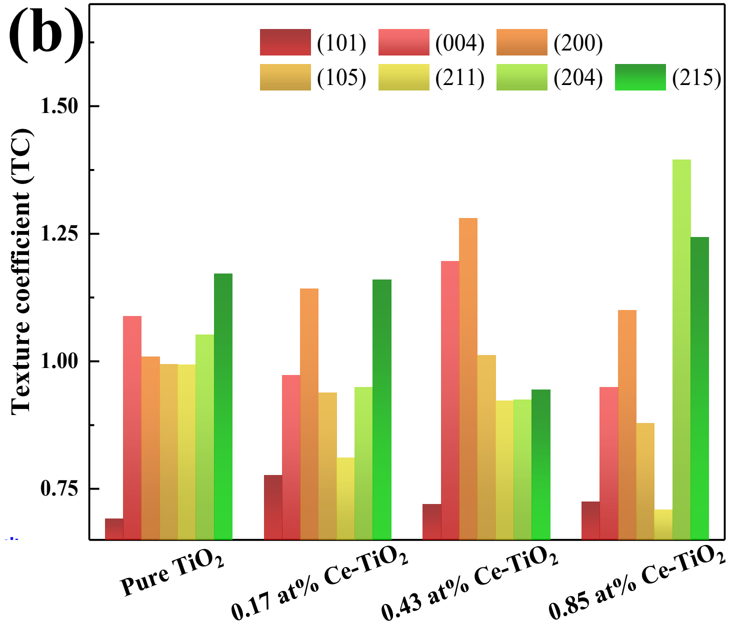

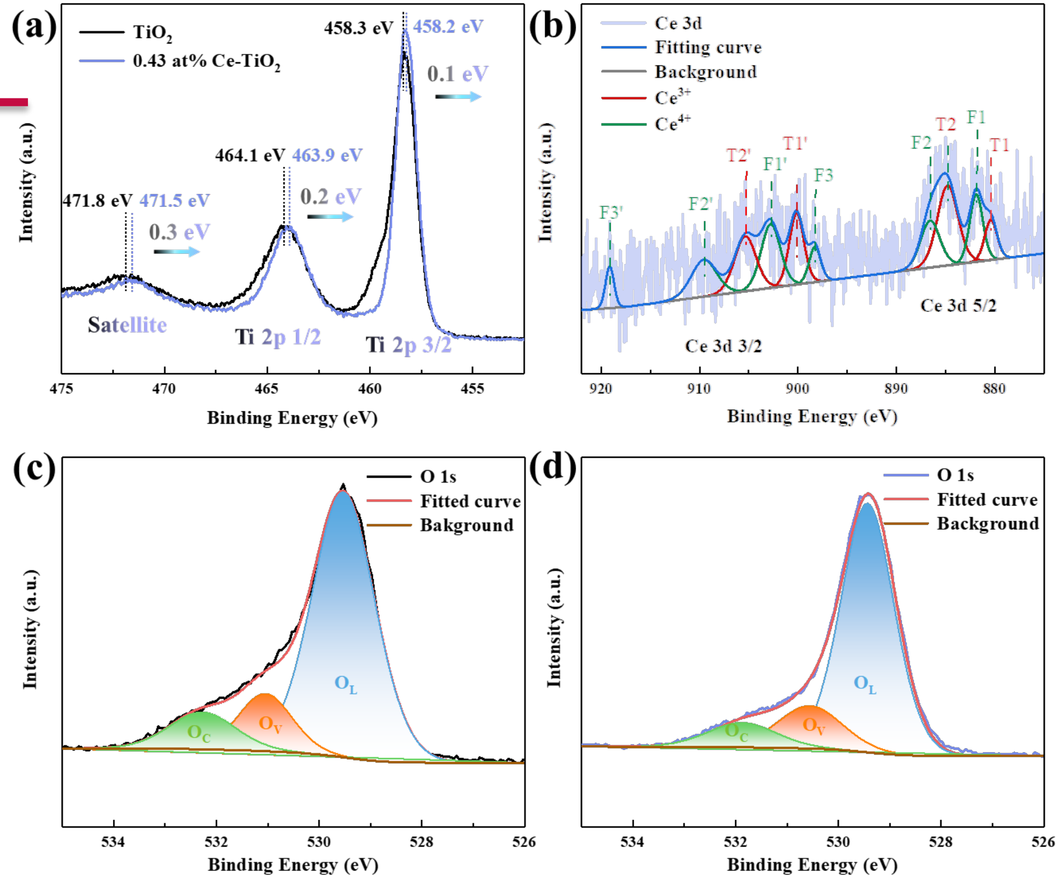

Sample	Grain size (nm)	$TC_{(101)}$	$TC_{(004)}$	$TC_{(200)}$	$TC_{(105)}$	$TC_{(211)}$	$TC_{(204)}$	$TC_{(215)}$
Pure TiO_2	6.1	0.6909	1.0885	1.0088	0.9944	0.9931	1.0523	1.1719
0.17 at% Ce-TiO_2	6.7	0.7771	0.9729	1.1421	0.9382	0.8108	0.9493	1.1596
0. 43 at% Ce-TiO_2	7.0	0.7195	1.1959	1.2808	1.0116	0.9232	0.9249	0.9442
0.85 at% Ce-TiO_2	7.9	0.7247	0.9495	1.0998	0.879	0.709	1.3952	1.243

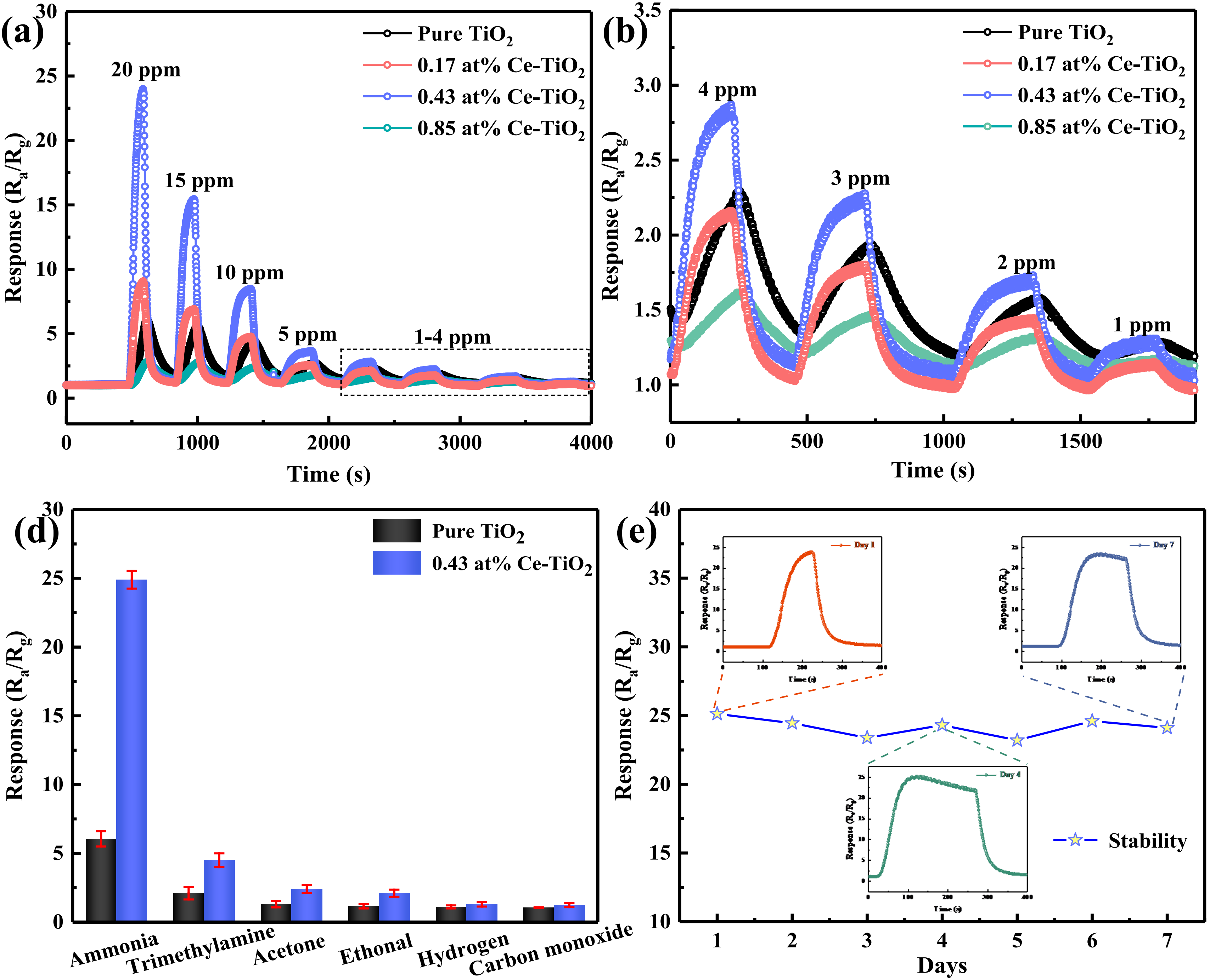

Fig. 2.1. (a) Dynamic response/recovery curves of three samples to 1–20 ppm NH_3. (b) responses values to 1–4 ppm NH_3. (c) responses/recovery time of 0.43 at% Ce-TiO_2 to 10 ppm NH_3 at room temperature. (d) Selectivity to 20 ppm NH_3 and various gases of 0.43 at% Ce-TiO_2 at RT. (e) Response stable characteristics of 0.43 at% Ce-TiO_2 sensor to 20 ppm NH_3 in one week.

Practical application

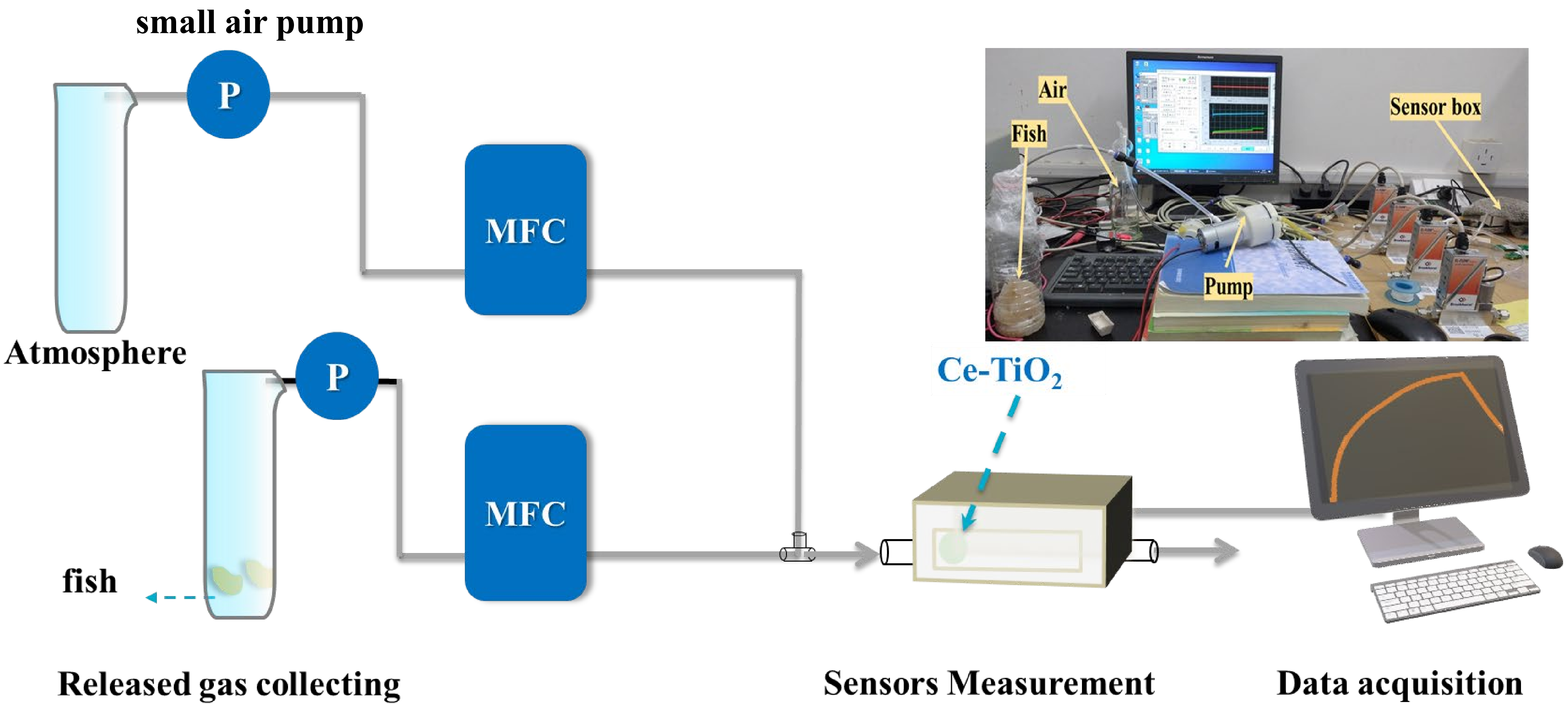

Scheme 2. Schematical diagram of the fish freshness detection system.

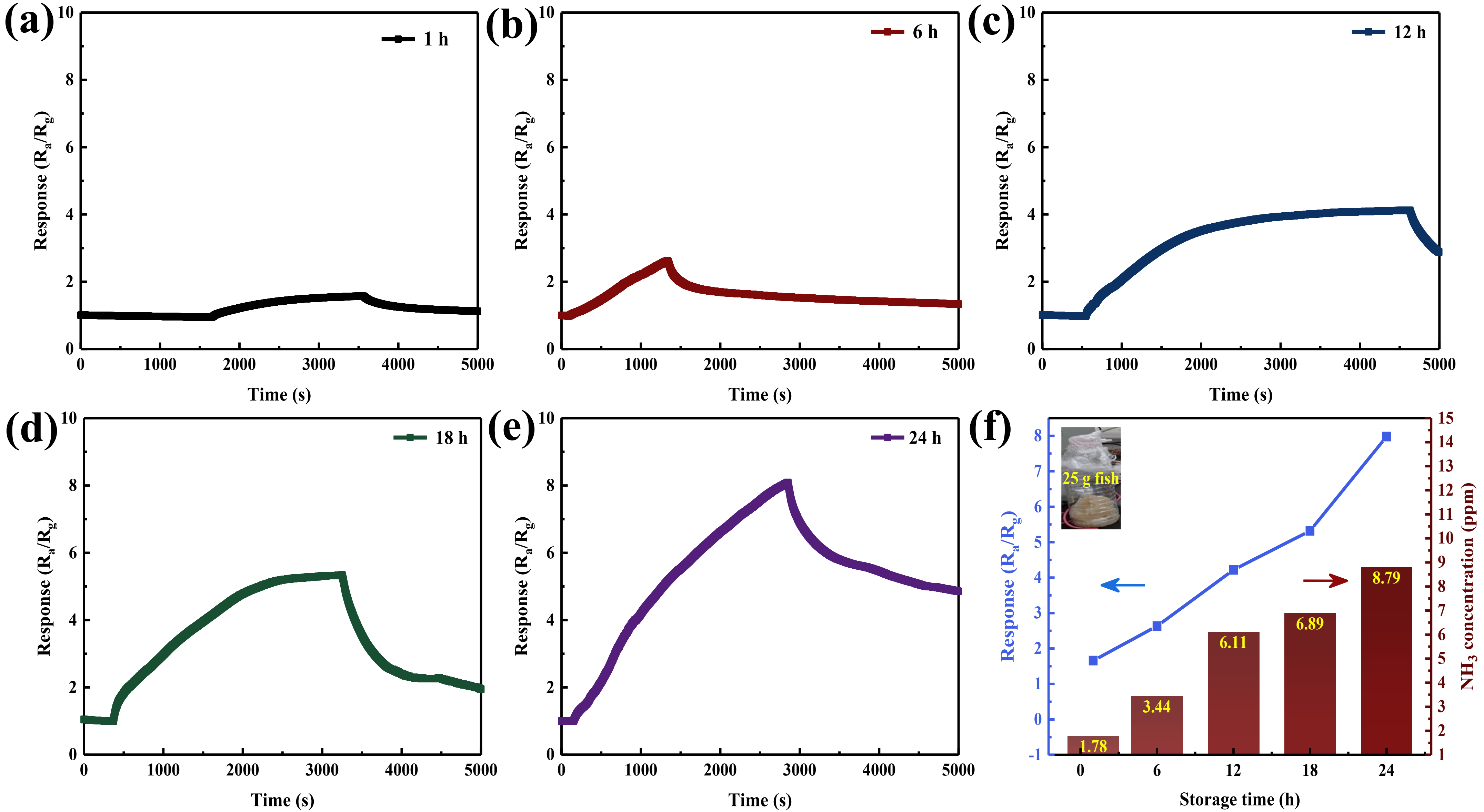

Fig. 2.2. Responses of the 0.43 at% Ce-TiO_2 gas sensor towards the released gases from 25 g Pangasius fillet during different stages (1, 6, 12, 18, 24 h).

Contents

Conclusions

1. A series of gas sensors based on metal oxides for detecting the released gases (H_2S and NH_3) during fish spoilage process were developed.
2. WO_3-Bi_2WO_6 microflowers based gas sensor showed good sensing properties to ppb-level H_2S.
3. Ce-TiO_2 nanocrystals showed good sensing properties to low-concentration NH_3.
4. The practical application potential of as-fabricated gas sensors was verified by detecting fish spoilage.

Contents

Next work

Mo-based TMA gas sensor— —ppm level（>10×10^{-6}）

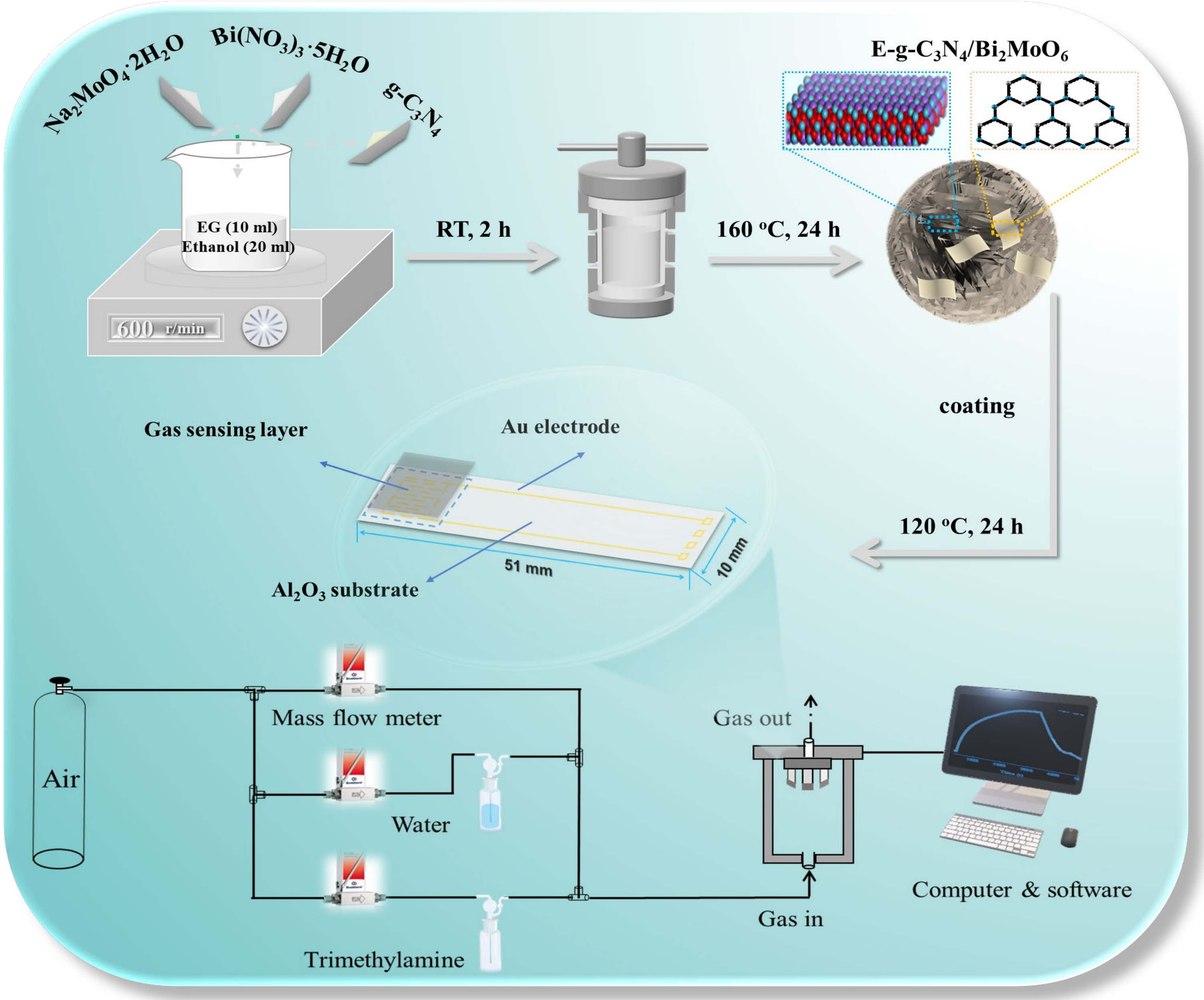

Gas sensing tests

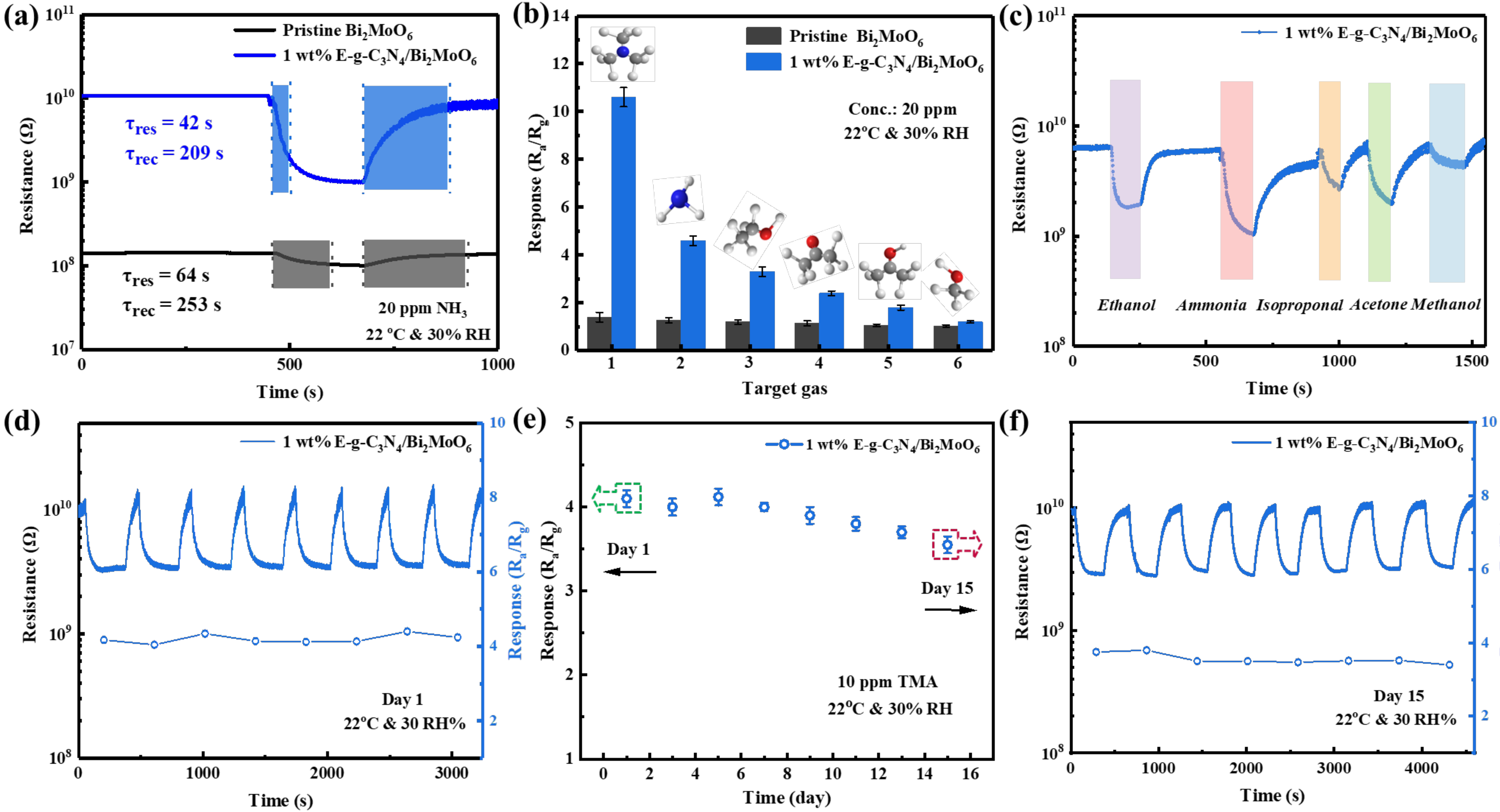

Practical application

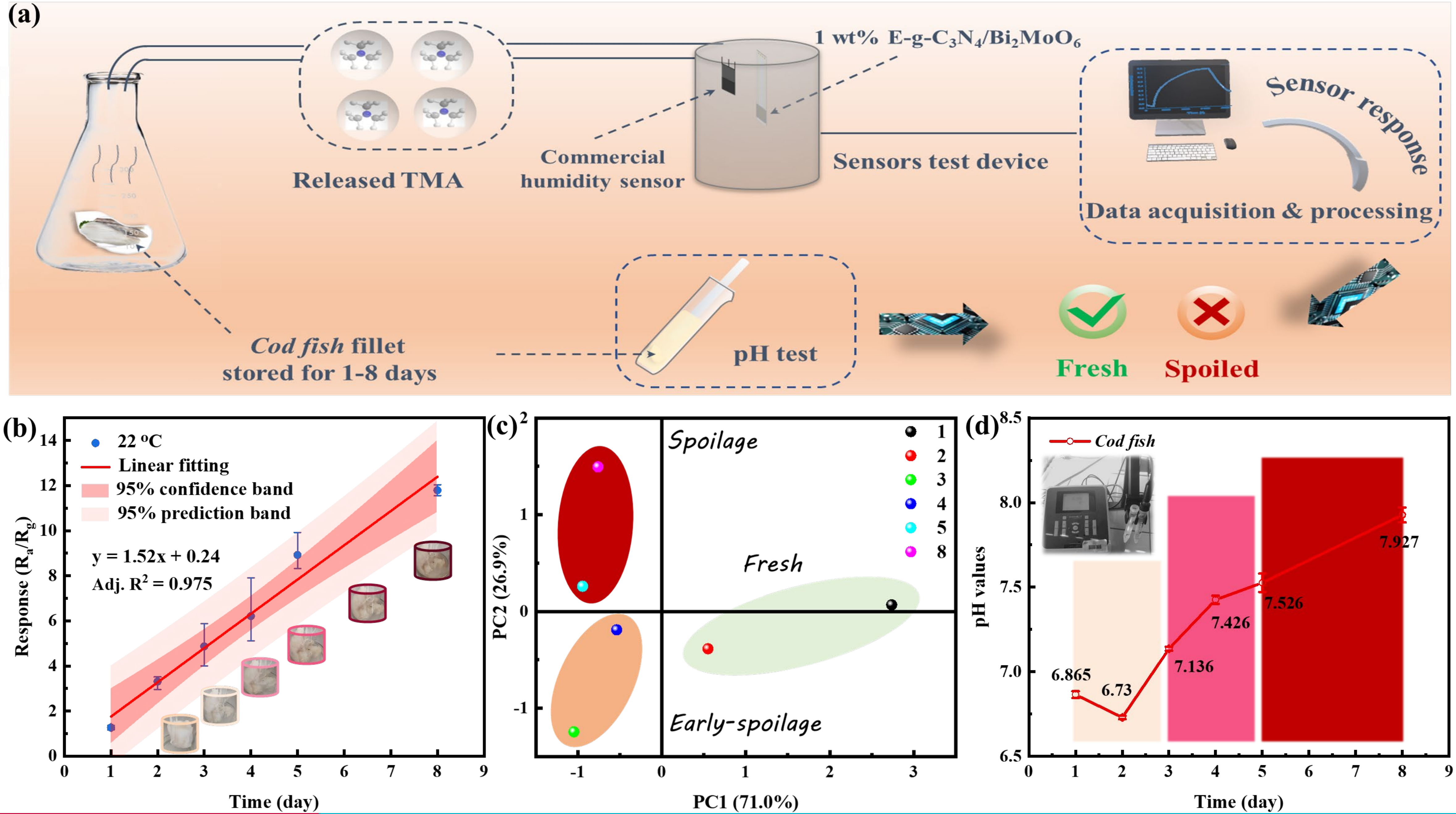

Acknowledgement

National Construction High-level University Public Postgraduate Program of China

Outstanding Doctoral Dissertation Fund Project of Yangzhou University

UMONS Université de Mons

materials UMONS RESEARCH INSTITUTE FOR MATERIALS SCIENCE AND ENGINEERING

揚州大學 YANGZHOU UNIVERSITY

国家留学基金管理委员会 CHINA SCHOLARSHIP COUNCIL

Thanks